Mid-Infrared Spectrum of $[Ru(bpy)_3]^{2+*}$

Kristin M. Omberg,[†] Jon R. Schoonover,*[,‡] Joseph A. Treadway,[†] Robert M. Leasure,[†] R. Brian Dyer,[‡] and Thomas J. Meyer*[,†]

Contribution from the Department of Chemistry,[§] University of North Carolina, Chapel Hill, North Carolina 27599-3290, and the Bioscience and Biotechnology Group (CST-4), Chemical Science and Technology Division, Mail Stop J586, Los Alamos National Laboratory, Los Alamos, New Mexico 87545

Received February 18, 1997[⊗]

Abstract: The first time-resolved infrared difference spectra for metal-to-ligand charge transfer (MLCT) excited states in the fingerprint region from 1400 to 1625 cm^{-1} are reported for $[Ru(bpy)_3]^{2+*}$ and $[Re(bpy)(CO)_3(4\text{-Etpy})]^{+*}$ in CD_3CN at 298 K (bpy is 2,2′-bipyridine; 4-Etpy is 4-ethylpyridine). The spectra are assigned by comparison to ground-state spectra and electrochemically generated $[Ru^{III}(bpy)_3]^{3+}$ and $[Ru^{II}(bpy^{\bullet-})(bpy)_2]^{+}$. The data provide clear evidence for the localized description $[Ru^{III}(bpy^{\bullet-})(bpy)_2]^{2+*}$ on the ∼100 ns time scale. They also give insight into electronic distribution in the excited state based on the magnitudes and directions of the infrared shifts.

Introduction

Vibrational spectroscopy has proven to be an invaluable tool for studying the metal-to-ligand charge transfer (MLCT) excited states of transition metal polypyridyl complexes.[1] These complexes are of interest because of their excited state properties and ability to undergo facile electron and energy transfer in molecular assemblies.[2] Since Dallinger and Woodruff first reported the time-resolved resonance Raman (TR^3) spectrum of the lowest MLCT excited state(s) of $[Ru(bpy)_3]^{2+}$ (bpy is 2,2′-bipyridine),[3] significant progress has been made in understanding ground- and excited-state vibrational structure. Kincaid and co-workers have reported normal-coordinate analyses for both ground- and excited-state $[Ru(bpy)_3]^{2+}$,[4] and a number of groups have analyzed excited-state structural changes based on ground-state resonance Raman (RR) data.[5] The Raman studies are of great value but only provide information about resonantly enhanced, symmetric vibrations. The significant amount of information available from infrared-active asymmetric modes remains untapped.

Time-resolved infrared (TRIR) spectroscopy complements resonance Raman.[6−8] It has been particularly useful for complexes with CO or CN ligands since these act as "reporters" on changes in electronic distribution between ground and excited states.[7] Continuing advances have made it possible to observe transient signals throughout the mid-infrared (4000−500 cm^{-1}) with high sensitivity ($\Delta OD < 10^{-4}$).[8] Time-resolved, step-scan Fourier transform infrared spectroscopy has proven to be especially advantageous on the nanosecond and slower time scales.[9] In this technique the moving mirror is held at a fixed

[†] University of North Carolina at Chapel Hill.

[‡] Los Alamos National Laboratory.

[§] Contribution No. 3290.

[⊗] Abstract published in *Advance ACS Abstracts,* July 1, 1997.

(1) (a) McClanahan, S.; Kincaid, J. R. *J. Raman Spectrosc.* **1984**, *15*, 173. (b) Caspar, J. V.; Westmoreland, T. D.; Allen, G. H.; Bradley, P. G.; Meyer, T. J.; Woodruff, W. H. *J. Am. Chem. Soc.* **1984**, *106*, 3492. (c) McClanahan, S. F.; Dallinger, R. F.; Holler, F. J.; Kincaid, J. R. *J. Am. Chem. Soc.* **1985**, *107*, 4853. (d) Mabrouk, P. A.; Wrighton, M. S. *Inorg. Chem.* **1986**, *25*, 526. (e) Kumar, C. V.; Barton, J. K.; Turro, N. J.; Gould, I. R. *Inorg. Chem.* **1987**, *26*, 1455. (f) Kumar, C. V.; Barton, J. K.; Gould, I. R.; Turro, N. J.; Van Houten, J. *Inorg. Chem.* **1988**, *27*, 648. (g) Doorn, S. K.; Hupp, J. T. *J. Am. Chem. Soc.* **1989**, *111*, 4704. (h) Yabe, T.; Anderson, D. R.; Orman, L. K.; Chang, Y. S.; Hopkins, J. B. *J. Phys. Chem.* **1989**, *93*, 2302. (i) Chang, Y. S.; Xu, X.; Yabe, T.; You, S.-C.; Anderson, D. R.; Orman, L. K.; Hopkins, J. B. *J. Phys. Chem.* **1990**, *94*, 729. (j) Yabe, T.; Orman, L. K.; Anderson, D. R.; You, S.-C.; Xu, X.; Hopkins, J. B. *J. Phys. Chem.* **1990**, *94*, 7128. (k) Maruszewski, K.; Badjor, K.; Strommen, D. P.; Kincaid, J. R. *J. Phys. Chem.* **1995**, *99*, 6286.

(2) (a) Crosby, G. A.; Highland, R. G.; Truesdell, K. A. *Coord. Chem. Rev.* **1985**, *64*, 41. (b) DeArmond, M. K.; Hanck, K. W.; Wertz, D. W. *Coord. Chem. Rev.* **1985**, *64*, 65. (c) Meyer, T. J. *Acc. Chem. Res.* **1989**, *22*, 163. (d) Scandola, R.; Indelli, M. T.; Chiorboli, C.; Bignozzi, C. A. *Top. Curr. Chem.* **1990**, *158*, 73. (e) Balzani, V.; Scandola, F. *Supramolecular Photochemistry*; Horwood: Chichester, U.K., 1991; Chapters 5 and 6. (f) Kalyanasundaram, K. *Photochemistry of Polypyridine and Porphyrin Complexes*; Academic Press: London, 1992.

(3) (a) Dallinger, R. F.; Woodruff, W. H. *J. Am. Chem. Soc.* **1979**, *101*, 4391. (b) Bradley, P. G.; Kress, N.; Hornberger, B. A.; Dallinger, R. F.; Woodruff, W. H. *J. Am. Chem. Soc.* **1981**, *103*, 7441.

(4) (a) Mallick, P. K.; Danzer, G. D.; Strommen, D. P.; Kincaid, J. R. *J. Phys. Chem.* **1988**, *92*, 5628. (b) Strommen, D. P.; Mallick, P. K.; Danzer, G. D.; Lumpkin, R. S.; Kincaid, J. R. *J. Phys. Chem.* **1990**, *94*, 1357.

(5) (a) Kober, E. M.; Meyer, T. J. *Inorg. Chem.* **1982**, *21*, 3978. (b) Smothers, W. K.; Wrighton, M. S. *J. Am. Chem. Soc.* **1983**, *105*, 1067. (c) Poizat, O.; Sourisseau, C. *J. Phys. Chem.* **1984**, *88*, 3007. (d) Chung, Y. L.; Leventis, N.; Wagner, P. J.; Leroi, G. E. *J. Am. Chem. Soc.* **1985**, *107*, 1416. (e) Carroll, P. J.; Brus, L. E. *J. Am. Chem. Soc.* **1987**, *109*, 7613. (f) Myers, A. B. *Chem. Rev.* **1996**, *96*, 911.

(6) Schoonover, J. R.; Bignozzi, C. A.; Meyer, T. J. *Coord. Chem. Rev.* In press.

(7) (a) Glyn, P.; George, M. W.; Hodges, P. M.; Turner, J. J. *J. Chem. Soc., Chem. Commun.* **1989**, 1655. (b) Doorn, S. K.; Gordon, K. C.; Dyer, R. B.; Woodruff, W. H. *Inorg. Chem.* **1992**, *31*, 2284. (c) Doorn, S. K.; Stoutland, P. O.; Dyer, R. B.; Woodruff, W. H. *J. Am. Chem. Soc.* **1992**, *114*, 3133. (d) Bignozzi, C. A.; Argazzi, R.; Schoonover, J. R.; Gordon, K. C.; Dyer, R. B.; Scandola, F. *Inorg. Chem.* **1992**, *31*, 5260. (e) Turner, J. J.; George, M. W.; Johnson, F. P. A.; Westwell, J. R. *Coord. Chem. Rev.* **1993**, *125*, 101. (f) Doorn, S. K.; Dyer, R. B.; Stoutland, P. O.; Woodruff, W. H. *J. Am. Chem. Soc.* **1993**, *115*, 6398. (g) Schoonover, J. R.; Gordon, K. C.; Argazzi, R.; Woodruff, W. H.; Peterson, K. A.; Bignozzi, C. A.; Dyer, R. B.; Meyer, T. J. *J. Am. Chem. Soc.* **1993**, *115*, 10996. (h) Schoonover, J. R.; Bates, W. D.; Strouse, G. F.; Chen, P.; Dyer, R. B.; Meyer, T. J. *Inorg. Chem.* **1995**, *35*, 273. (i) Strouse, G. F.; Schoonover, J. R.; Duesing, R.; Meyer, T. J. *Inorg. Chem.* **1995**, *34*, 2725. (j) Schoonover, J. R.; Strouse, G. F.; Omberg, K. M.; Dyer, R. B. *Comments Inorg. Chem.* **1995**, *18*, 165.

(8) (a) Dyer, R. B.; Killough, P. M.; Einarsdóttir, Ó.; López-Garriga, J. J.; Woodruff, W. H. *J. Am. Chem. Soc.* **1989**, *111*, 7657. (b) Dyer, R. B.; López-Garriga, J. J.; Einarsdóttir, Ó.; Woodruff, W. H. *J. Am. Chem. Soc.* **1989**, *111*, 8962. (c) Stoutland, P. O.; Dyer, R. B.; Woodruff, W. H. *Science* **1992**, *257*, 1913. (d) Li, M.; Owrutsky, J.; Sarisky, M.; Culver, J. P.; Yodh, A.; Hochstrasser, R. M. *J. Chem. Phys.* **1993**, *98*, 5499. (e) Raftery, D.; Iannone, M.; Phillips, C. M.; Hochstrasser, R. M. *Chem. Phys. Lett.* **1993**, *201*, 513. (f) Wynne, K.; Hochstrasser, R. M. *Chem. Phys.* **1995**, *193*, 211.

(9) (a) Palmer, R. A.; Manning, C. J.; Rzepiela, J. A.; Widder, J. M.; Chao, J. L. *Appl. Spectrosc.* **1989**, *43*, 193. (b) Uhmann, W.; Becker, A.; Taran, C.; Siebert, F. *Appl. Spectrosc.* **1991**, *45*, 390. (c) Palmer, R. A. *Spectroscopy* **1993**, *8*, 26. (d) Palmer, R. A.; Chao, J. L.; Dittmar, R. M.; Gregoriou, V. G.; Plunkett, S. E. *Appl. Spectrosc.* **1993**, *47*, 1297. (e) Weidlich, O.; Siebert, F. *Appl. Spectrosc.* **1993**, *47*, 952.

S0002-7863(97)00511-8 CCC: $14.00

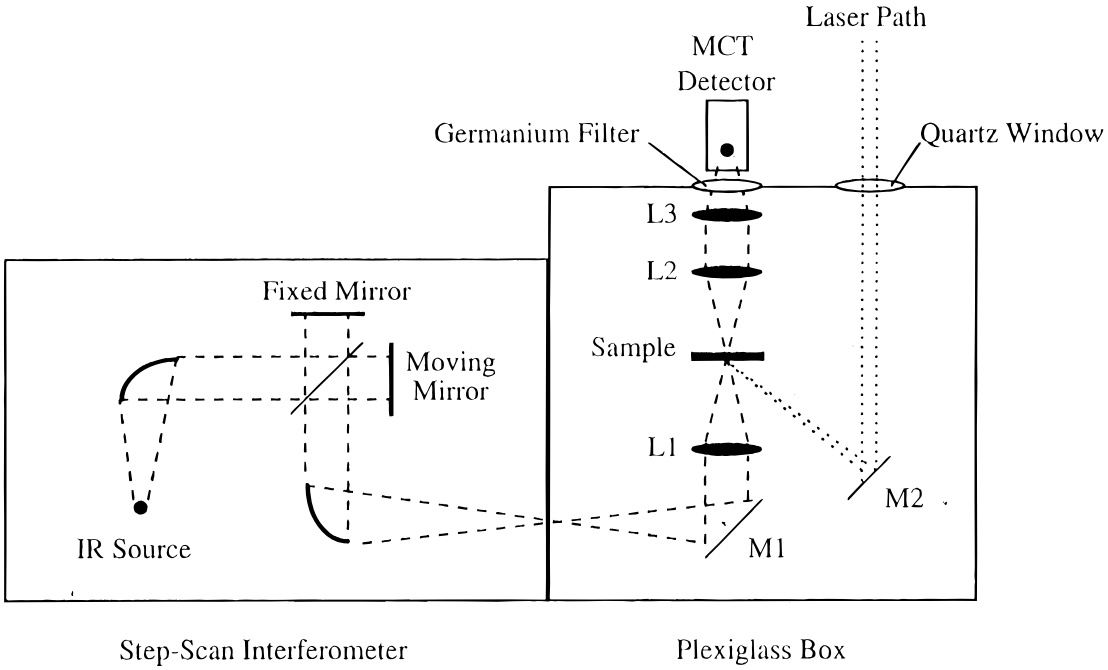

Figure 1. Optical layout of the time-resolved, step-scan FTIR spectrometer.

position while a transient is repetitively produced by pulsed laser excitation. The mirror is stepped to the next position and the process repeated. This produces a temporally digitized transient signal at each discrete mirror position. The data are manipulated to give a series of interferograms, then transient spectra.

The measurement of TR[3] spectra requires resonance enhancement by an electronic transition of the excited state. For $[Ru(bpy)_3]^{2+*}$ the $\pi \rightarrow \pi^*$ absorption near 370 nm provides a convenient transition, with selective enhancement occurring only for those vibrations for which there is a change in equilibrium displacement between states.[3,4b] In contrast, in TRIR there is no selective enhancement. The *difference* in absorption between the excited state or intermediate and the ground state is observed, and all IR-active bands which undergo a change in energy or intensity contribute to the spectrum.

We report here the first application of TRIR to the lowest MLCT excited states of $[Ru(bpy)_3]^{2+}$ and $[Re(bpy)(CO)_3(4\text{-Etpy})]^+$ (4-Etpy is 4-ethylpyridine) in the IR fingerprint region from 1400 to 1625 cm^{-1}. Ligand-based polypyridyl vibrations dominate this region[4] and provide important information about the chromophoric and nonchromophoric ligands in the excited state.

Experimental Section

Materials. Unless otherwise noted, all solvents and materials were used as received, without additional purification. Acetonitrile-d_3 was purchased from Cambridge Isotope Labs. Acetonitrile was obtained from Burdick and Jackson. Perchloric acid was purchased from GFS. Tetra-*n*-butylammonium hexafluorophosphate (TBAH) was obtained from Aldrich and recrystallized twice from ethanol. Ceric ammonium nitrate was purchased from Sigma. $[Ru(bpy)_3](PF_6)_2$[10] and $[Re(CO)_3(bpy)(4\text{-Etpy})](CF_3SO_3)$[11] were prepared according to literature methods.

Infrared Measurements. A BioRad FTS 60A/896 step-scan interferometer served as the IR source. As shown in Figure 1, the IR beam from the interferometer was directed out of a sampling port on the instrument to mirror M1, which directed the light to calcium fluoride lens L1. Lens L1 tightly focused the IR beam onto the sample; the diameter of the beam at the sample was between 300 and 500 μm. The IR light was collected by lens L2 (calcium fluoride) and then focused by lens L3 (calcium fluoride) onto the element of a photoconductive mercury cadmium telluride (MCT) detector (Graesby Infrared). A low-pass germanium optical filter (2250 cm^{-1}) was attached to the face of the MCT detector to block emission from the sample and prevent saturation of the detector by filtering out IR radiation outside the region of interest. The combination of the filter and calcium fluoride optics allowed a nominal spectra range of 1250 to 2250 cm^{-1}. Deuterated acetonitrile provided a practical solvent window above 1300 cm^{-1}. Due to signal-to-noise considerations the effective sampling window was 1400−2250 cm^{-1}. Acetonitrile provided a practical solvent window throughout the carbonyl region (1700−2200 cm^{-1}). The optical train was enclosed in a plexiglass box purged by a continuous flow of nitrogen.

For ground-state FTIR spectra, the interferometer was operated in the conventional rapid-scan mode. The signal from the MCT detector was amplified by a DC-coupled preamplifier and processed by the interferometer. A 1 mm path length sealed sample cell with CaF_2 windows was used. All ground-state spectra reported are an average of 64 scans with 4-cm^{-1} resolution.

For TRIR spectra, the interferometer was operated in step-scan mode. The sample was excited with the third harmonic (354.7 nm) of a Q-switched Nd:YAG laser (Spectra-Physics DCR-11, 10 ns pulse width). The pump beam was focused to less than a 10-mm diameter at the sample with a power of between 100 and 200 μJ per pulse. The beam was directed into the sample chamber through a quartz window and onto the sample cell by mirror M2 (Figure 1). The pump beam and IR beam were overlapped with a pinhole in place of the sample. The signal from the MCT detector was amplified by a DC-coupled preamplifier and processed in two matched boxcar integrators (Stanford Research Systems, Model SR250).

The gate of one boxcar was placed at time zero. Initial placement was accomplished by overlapping the gate with the laser signal from a photodiode. Final adjustment was made with the signal output. This gate corresponded to the excited-state, or light-on, signal. The gate of the second boxcar was placed 62.5 μs before time zero to collect the ground-state, or light-off, signal. This exact timing sequence was necessary to synchronize the phase of the 16-kHz moving mirror dither. The dither of the moving mirror was used to provide feedback control for mirror positioning. The dither produced an infrared transient at the fixed frequency of the dither that had a large amplitude compared to that of a typical laser-induced transient, and acted as a significant noise source unless it was demodulated from the transient spectrum.

(10) (a) Sullivan, B. P.; Salmon, D. J.; Meyer, T. J. *Inorg. Chem.* **1977**, *17*, 3334. (b) Caspar, J. V.; Meyer, T. J. *J. Am. Chem. Soc.* **1983**, *105*, 5583.

(11) Worl, L. A.; Duesing, R.; Chen, P.; Della Ciana, L.; Meyer, T. J. *J. Chem. Soc., Dalton Trans.* **1991**, *849*.

Table 1. Infrared Band Energies (cm^{-1}) for $[Ru^{II}(bpy)_3]^{2+}$, $[Ru(bpy)_3]^{2+}$*, $[Ru^{II}(bpy)_2(bpy^{\bullet-})]^{+}$, and $[Ru^{III}(bpy)_3]^{3+}$ in Acetonitrile-d_3 at 298 K

$[Ru^{II}(bpy)_3]^{2+}$	$[Ru(bpy)_3]^{2+}$*	$[Ru^{II}(bpy)_2(bpy^{\bullet-})]^{+}$ [a]	$[Ru^{III}(bpy)_3]^{3+}$ [b]	$[Ru^{III}(bpy)_3]^{3+}$[c]
1604	1608		1602	
	1548	1541		
	1500		1496	
1487[d]	1490	1488		
1466	1469		1471	1471
	1462	1465		
1447	1449	1446		
	1444		1440	1442
1425	1427		1425	1426
	1420	1418		

[a] Electrochemically generated. Bands corresponding to $[Ru^{II}(bpy)_3]^{2+}$ are also observed from the unreduced bipyridine ligands. [b] Electrochemically generated. [c] Chemically generated; the spectral window ends at 1485 cm^{-1} due to water in the sample. [d] Shoulder.

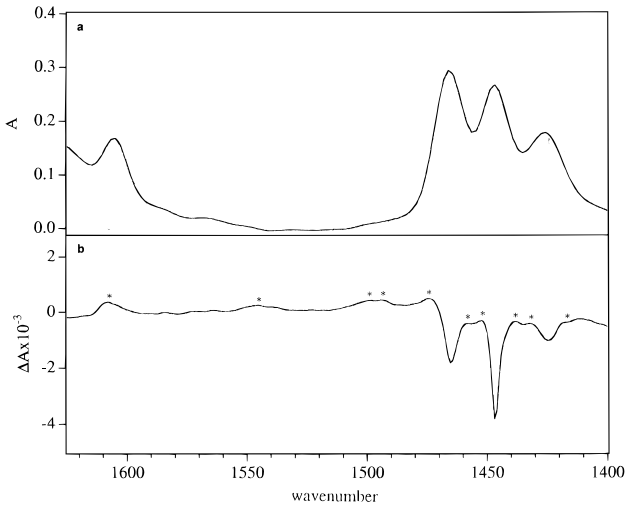

Figure 2. Ground-state (a) and TRIR (b) spectra of $[Ru(bpy)_3]^{2+}$ in acetonitrile-d_3 at 298 K. Excited state bands are labeled with an asterisk.

The width of both gates was set at 450 ns. The laser repetition rate, interferometer step rate, and boxcar integration were synchronized at 10 Hz with a digital delay generator (Stanford Research Systems, Model DG 535). The stepping signal from the interferometer was the master clock that triggered the delay generator, which in turn triggered the laser and the boxcars. The two integrated signals from the boxcars produced "dark" (light-off) and "light" (light-on) single-beam spectra in the interferometer software. The transient difference spectrum was computed as $\Delta A = -\log(\text{light/dark})$. All time-resolved spectra shown are an average of 256 scans at 4-cm^{-1} resolution except for the carbonyl-region spectrum, which is an average of 32 scans.

Samples for TRIR Studies. All fingerprint-region spectra were acquired in acetonitrile-d_3. The carbonyl-region spectrum was acquired in acetonitrile. Sample concentrations were adjusted to give an absorbance of approximately 0.7 for the most intense bipyridine bands, or 1.0 for the CO bands when examining the carbonyl region. The sample cell and sample solutions were deoxygenated by sparging with argon for 15 min; solutions were transferred to the cell under an inert atmosphere. Spectra were acquired in blocks of 16 scans for $[Re(bpy)(CO)_3(4\text{-Etpy})]^{+}$ and in blocks of 64 scans for $[Ru(bpy)_3]^{2+}$ to ensure sample integrity.

$[Ru^{III}(bpy)_3]^{3+}$ and $[Ru^{II}(bpy)_2(bpy^{\bullet-})]^{+}$. These ions were generated by bulk electrolysis of $[Ru^{II}(bpy)_3]^{2+}$ in acetonitrile-d_3 with 0.1 M TBAH as the electrolyte. The solutions used were 0.01 M in $[Ru^{II}(bpy)_3]^{2+}$, giving an infrared absorbance of ~0.5 for the most intense bipyridine bands. The reduced and oxidized forms were prepared by quantitative reduction (at −1.7 V vs SSCE) and oxidation (at 1.5 V vs SSCE) with platinum working and counter electrodes and a $Ag/AgNO_3$ reference electrode in a standard three-compartment cell. $[Ru^{III}(bpy)_3]^{3+}$ was also prepared chemically in acetonitrile-d_3 by oxidation with 1 equiv of 0.1 M ceric ammonium nitrate in 2 M perchloric acid. Samples were prepared and transferred to the sample cell under an inert atmosphere. Spectra were measured on a Mattson Galaxy Series FTIR spectrometer in a 0.25 mm path length cell with calcium fluoride windows.

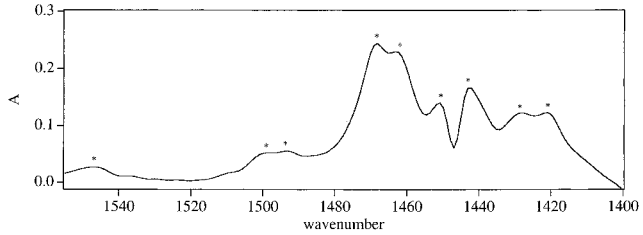

Figure 3. Absorption spectrum of $[Ru(bpy)_3]^{2+}$* in acetonitrile-d_3 at 298 K, calculated as described in the text. Excited state bands are labeled with an asterisk.

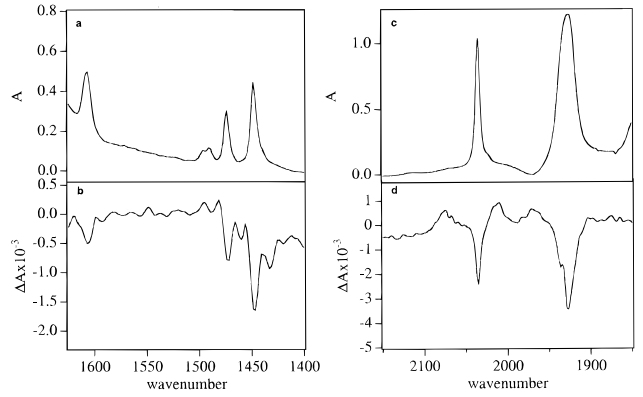

Figure 4. Ground-state (a, c) and TRIR (b, d) spectra of $[Re(bpy)(CO)_3(4\text{-Etpy})]^{+}$ in the bipyridine (a, b) and carbonyl (c, d) regions in acetonitrile-d_3 at 298 K.

Results

The ground-state and time-resolved infrared difference (FTIR) spectra of $[Ru(bpy)_3]^{2+}$ between 1400 and 1625 cm^{-1} are shown in Figure 2. Five bands are observed in the ground-state spectrum; ten can be discerned in the transient spectrum. The band energies are listed in Table 1. The ground-state infrared band energies between 1400 and 1625 cm^{-1} for $[Ru^{III}(bpy)_3]^{3+}$ (generated both electrochemically and chemically in acetonitrile-d_3) and $[Ru^{II}(bpy)_2(bpy^{\bullet-})]^{+}$ (generated electrochemically in acetonitrile-d_3) are also listed in Table 1. Five major bands are observed in each spectrum. An excited-state absorption spectrum (A_{ES}) for $[Ru(bpy)_3]^{2+}$* was calculated by adding the ground-state spectrum (A_{GS}) to the weighted difference spectrum (A_{TRIR}) according to the following equation, $A_{ES} = 100A_{TRIR} + A_{GS}$. The result is shown in Figure 3.

Ground-state and TRIR spectra of $[Re(bpy)(CO)_3(4\text{-Etpy})]^{+}$ in the ν(CO) region and from 1400 to 1625 cm^{-1} are shown in Figure 4. Six bands are observed in the ground-state spectrum from 1400 to 1625 cm^{-1}, and eight in the transient spectrum. The energies of these bands are listed in Table 2.

Infrared band energies and assignments for $[Ru(bpy)_3]^{2+}$* and $[Re(bpy)(CO)_3(4\text{-Etpy})]^{+}$* are given in Table 3.

Table 2. Ground- and Excited-State Infrared Band Energies in cm^{-1} for $[Re(bpy)(CO)_3(4\text{-Etpy})]^+$ in Acetonitile-d_3 at 298 K

$[Re^I(bpy)(CO)_3(4\text{-Etpy})]^+$	$[Re(bpy)(CO)_3(4\text{-Etpy})]^{+}*$
1607	1547
	1524
	1516
1497[a]	1494
1491	1483
1474	1466
1449	1454
1429[b]	1425

[a] Shoulder. [b] 4-Ethylpyridine band.

Table 3. Mid-IR Band Energies (cm^{-1}) and Proposed Origins for $[Ru(bpy)_3]^{2+}*$ and $[Re(bpy)(CO)_3(4\text{-Etpy})]^{+}*$ in Acetonitrile-d_3 at 298 K

$[Ru(bpy)_3]^{2+}*$	$[Re(bpy)(CO)_3(4\text{-Etpy})]^{+}*$	origin
1608		Ru^{III}(bpy)
1548	1547	$bpy^{\bullet-}$
	1524	4-Etpy
1500	1494	$bpy^{\bullet-}$
1490		Ru^{III}(bpy)
	1483	4-Etpy
1469		Ru^{III}(bpy)
1462	1466	$bpy^{\bullet-}$
1449	1454	$bpy^{\bullet-}$
1444		Ru^{III}(bpy)
1427		Ru^{III}(bpy)
1420	1425	$bpy^{\bullet-}$

Discussion

Analysis of the Spectra. The data presented here for $[Ru(bpy)_3]^{2+}*$ and $[Re(bpy)(CO)_3(4\text{-Etpy})]^{+}*$ represent the first application of TRIR to the fingerprint region for MLCT excited states. When combined with the normal coordinate analyses of ground- and excited-state $[Ru^{II}(bpy)_3]^{2+}$, these results provide significant insight into excited state molecular and electronic structure.

From the results of earlier spectroscopic and temperature-dependent lifetime measurements, the MLCT excited "states" of $[Ru(bpy)_3]^{2+}$ and $[Re(bpy)(CO)_3(4\text{-Etpy})]^+$ are actually composites of three low-lying states.[12,13] All share the $d\pi^5\pi^{*1}$ electronic configuration and are largely triplet in character. At temperatures above 100 K all are appreciably populated and room temperature TR[3] or TRIR spectra are Boltzmann-weighted averages of all three.

Kincaid and co-workers have analyzed the ground-state infrared, resonance Raman (RR), and time-resolved resonance Raman (TR[3]) spectra of $[Ru^{II}(bpy)_3]^{2+}$ and its deuteriated and ^{15}N-substituted analogs.[4] The spectra are dominated by bands that are primarily bipyridine ring-stretching modes. They can be interpreted by invoking a single coordinated bipyridine acceptor and C_{2v} symmetry. There are 57 normal modes for a single bipyridine ligand: 20 of A_1 symmetry, 9 of A_2 symmetry, 9 of B_1 symmetry, and 19 of B_2 symmetry. In theory, the A_1, B_1, and B_2 modes are IR active, and all modes are Raman active. In practice, the totally symmetric A_1 modes are extremely weak in the IR, but selectively enhanced in the resonance Raman. Because of this, RR and TR[3] spectra are dominated by bands arising from the A_1 modes, and IR and TRIR spectra by bands from the B_2 modes. The A_1 and B_2 modes in the ground state and A_1 modes in the excited state have been assigned as combinations of local stretching and bending modes.[4] These assignments have been used to calculate predicted band energies and potential energy distributions (PEDs) for ground-state IR bands and ground- and excited-state Raman bands.

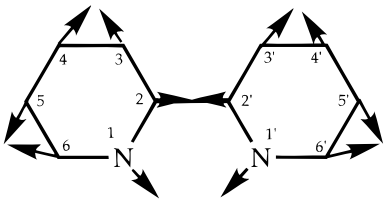

Figure 5. Predicted distortion of the acceptor 2,2′-bipyridine ligand in the MLCT excited state(s).[14]

Force constants have also been derived for the local stretching and bending contributors to the A_1 modes in the ground and excited states, assuming a single bipyridine acceptor ligand.[4] Changes in local mode force constants between ground and excited states and the PEDs of the normal modes provide a basis for predicting the magnitude and direction of the Raman shifts in the excited state. This assumes that local mode compositions do not vary significantly between states. This assumption is known to be valid for the Raman-active bands.[4] Given the similarities between the compositions of the A_1 and B_2 modes, it should be a reasonable assumption for the infrared bands as well. With this assumption, it is possible to use the force constant changes and PEDs to predict the directions and magnitudes of the IR band shifts in the excited state.

A molecular orbital analysis has also been used to predict structural changes in the bipyridyl acceptor ligand based on changes in LCAO coefficients between states.[14] The results of this analysis, which are illustrated in Figure 5, provide a second, qualitative method for analyzing IR shifts in the excited state.

Assignments for the five ground-state infrared bands of $[Ru(bpy)_3]^{2+}$ and $[Re(bpy)(CO)_3(4\text{-Etpy})]^+$ between 1400 and 1625 cm^{-1} are listed in Table 4. Calculated PEDs and changes in local mode force constants between ground and excited states are also given. The numbering scheme used to designate the bipyridyl local modes is illustrated in Figure 5.

These data, and the molecular orbital analysis provide a basis for accounting for the directions and magnitudes of infrared band shifts in the excited states. For example, the ground-state bipyridine band at 1604 cm^{-1} for $[Ru(bpy)_3]^{2+}$ is predicted to shift to lower energy in the excited state since its composition is dominated by $\nu(C_2-C_3)$.[4] The C_2-C_3 bond is a major contributor to the lowest π^* orbital, and the local stretching mode undergoes a substantial decrease in force constant in the excited state.[4,14] Other predicted changes include the following:

(1) The ground-state band at 1487 cm^{-1} shifts to higher energy because of enhanced $C_2-C_{2'}$ bonding and an increase in the $\nu(C_2-C_{2'})$ force constant in the excited state.

(2) The band at 1466 cm^{-1} shifts to lower energy due to the lengthening of C_4-C_5 and the decrease in the $\nu(C_4-C_5)$ force constant in the excited state.

(3) The 1447-cm^{-1} band shifts to higher energy because of the large contribution from $\nu(C_2-C_{2'})$ and enhanced $C_2-C_{2'}$ bonding.

(4) The band at 1425 cm^{-1} shifts to lower energy because of the contribution from $\nu(C_2-C_3)$.

Assignment of the Excited-State Spectrum of $[Re(bpy)(CO)_3(4\text{-Etpy})]^+$. Band energies for the ground and excited states of $[Re(bpy)(CO)_3(4\text{-Etpy})]^+$ are listed in Table 2. Since this complex possesses only one bpy ligand, correlation of the

(12) (a) Hager, G. D.; Crosby, G. A. *J. Am. Chem. Soc.* **1975**, *97*, 7031. (b) Hager, G. D.; Watts, R. J.; Crosby, G. A. *J. Am. Chem. Soc.* **1975**, *97*, 7037. (c) Kober, E. M.; Meyer, T. J. *Inorg. Chem.* **1984**, *23*, 3877.

(13) Striplin, D. R.; Crosby, G. A. *Chem. Phys. Lett.* **1994**, *221*, 426.

(14) Kober, E. M.; Meyer, T. J. *Inorg. Chem.* **1985**, *24*, 106.

Table 4. Ground-State Potential Energy Distributions (PEDs, in %) and Local Mode Force Constant Changes in the MLCT Excited States of $[Ru(bpy)_3]^{2+}$ (Ru(bpy)) and $[Re(bpy)(CO)_3(4\text{-Etpy})]^+$ (Re(bpy)) for the B_2 Modes Corresponding to Infrared Bands between 1400 and 1625 cm^{-1} (ref 4)

band energy (cm^{-1})					
Ru(bpy)	Re(bpy)	assignment	PED, %		ΔFC^a
1604	1607	ν_{25}	$\nu(C_2-C_3)$	46	−1.685
			$\nu(C-N)$	23	−0.261 (−0.103)[b]
1487	1491	$\nu_{18}+\nu_{33}$	ν_{18}: $\nu(M-N)$	25	0[c]
			$\nu(C_2-C_{2'})$	16	+1.087
			$\alpha(CCC)$	12	*d*
			$\nu(C-N)$	11	−0.261 (−0.103)
			ν_{33}: $\delta(CCH)$	35	−0.0092
			$\nu(C_3-C_4)$	13	+0.080
			$\alpha(CCC)$	11	*d*
1466	1474	ν_{27}	$\delta(C_2C_3H)$	28	−0.0055
			$\delta(CCH)$	25	−0.0092
			$\nu(C_4-C_5)$	21	−1.415
			$\nu(C-N)$	14	−0.261 (−0.103)
1447	1449	$\nu_{18}+\gamma(CH)$	ν_{18}: $\nu(M-N)$	25	0
			$\nu(C_2-C_{2'})$	16	+1.087
			$\alpha(CCC)$	12	*d*
			$\nu(C-N)$	11	−0.261 (−0.103)
1425	1427	ν_{28}	$\delta(CCH)$	47	−0.0092
			$\nu(C_2-C_3)$	28	−1.685
			$\delta(C_2C_3H)$	14	−0.0055

[a] ΔFC = ground state force constant − ^{3}MLCT state force constant. All stretching force constants are in mdyn/Å, bending constants are in (mdyn/Å)/ rad^{-2}, and stretch−bend interactions are in mdyn/rad. The numbering scheme for the local modes is shown in Figure 5 with designations such as $\nu(C_2-C_3)$ including contributions from both rings, $\nu(C_2-C_3)$ and $\nu(C_2'-C_3')$. [b] Either value may apply; the unspecified stretch could be $\nu(C_2-N)$ or $\nu(C_6-N)$. [c] Assumed to be zero. [d] Force constants not calculated; the $\alpha(CCC)$ local mode does not appear in the A_1 modes.

ground- and excited-state bands is straightforward. The correlations are as follows:

ground state, cm^{-1}	excited state, cm^{-1}
1607	1547
1491	1494
1474	1466
1449	1454
1429	1425

The remaining excited-state bands at 1524 and 1483 cm^{-1} are 4-ethylpyridine-based bands which appear at 1497 and 1455 cm^{-1} in the ground state. The shift to higher energy in these two bands is a secondary effect due to partial oxidation at the metal in the $[Re^{II}(bpy^{\bullet-})]$ excited state. This decreases electron density at Re, and with it, $d\pi(Re) \rightarrow \pi^*(4\text{-Etpy})$ back-bonding.

Except for ν_{25} at 1607 cm^{-1}, bipyridyl band shifts in the TRIR are small compared to the analogous Raman shifts; the magnitudes of the Raman shifts in this region vary from 4 (ν_7) to 60 cm^{-1} (ν_5).[3,4] This is expected since the infrared-active modes are nontotally-symmetric B_2 modes and do not participate significantly in the structural changes that occur at bpy upon excitation. Only the Raman-active, totally symmetric A_1 modes are integral to the excited-state distortion, and bands from these modes show considerable energy shifts in the excited state.

In the ν(CO) region (1900−2200 cm^{-1}), CO shifts for $[Re(bpy)(CO)_3(4\text{-Etpy})]^{+}$* (+39, +83, and +44 cm^{-1}) are consistent with partial oxidation of Re^I to Re^{II} in the excited state. Band energies increase because of decreased Re−CO back-bonding which increases the triple bond character of bound CO. Related observations have been made for the MLCT excited states of $[Re(phen)(CO)_3(4\text{-Mepy})]^+$ (4-Mepy is 4-methylpyridine)[7j] and $[Re(4,4'\text{-bpy})_2(CO)_3(Cl)]^+$ (4,4′-bpy is 4,4′-bipyridine).[7a,e]

The shifts in ν(CO) and the 4-Etpy and bpy bands in the excited state provide insight into electronic distribution. As noted above, decreased electron density at Re causes positive shifts in ν(CO) and ν(4-Etpy). Shifts in the bipyridine bands are consistent with partially reduced bpy. Both are consistent with the MLCT description $[Re^{II}(bpy^{\bullet-})(CO)_3(4\text{-Etpy})]^{+}$*. There is no evidence in the excited state for discrete contributions from the three low-lying MLCT states, all of which are appreciably populated at room temperature.[13] They share the same electronic configuration and must have comparable excited-state IR shifts.

Assignment of the Excited-State Spectrum of $[Ru(bpy)_3]^{2+}$. Ten infrared bands are observed between 1400 and 1625 cm^{-1} in the TRIR spectrum of $[Ru(bpy)_3]^{2+}$*. One set of five bands arises from the partially reduced acceptor ligand and can be assigned by comparison with $[Re(bpy)(CO)_3(4\text{-Etpy})]^{+}$* bands. The second set of five bands can be assigned to the ancillary bipyridine ligands which are only slightly shifted in the excited state.

In analyzing the spectrum of $[Ru(bpy)_3]^{2+}$*, it is also useful to make comparisons with the FTIR spectra of $[Ru^{III}(bpy)_3]^{3+}$ and $[Ru^{II}(bpy)_2(bpy^{\bullet-})]^+$. From the data in Table 1, bands for $[Ru^{II}(bpy)_2(bpy^{\bullet-})]^+$ are observed at 1541, 1488, 1465, 1446, and 1418 cm^{-1}. They correspond to bands in the TRIR spectrum of $[Re(bpy)(CO)_3(4\text{-Etpy})]^{+}$* at 1547, 1494, 1466, 1454, and 1425 cm^{-1}. All can be assigned as $bpy^{\bullet-}$ bands. In $[Ru(bpy)_3]^{2+}$*, there are corresponding bands at 1548, 1500, 1462, 1449, and 1420 cm^{-1}.

In the spectrum of $[Ru^{III}(bpy)_3]^{3+}$, bands appear at 1602, 1496, 1471, 1442, and 1425 cm^{-1}. They correspond to the remaining bands in the spectrum of $[Ru(bpy)_3]^{2+}$* at 1608, 1490, 1469, 1444, and 1427 cm^{-1}. They originate from the ancillary bpy ligands in the MLCT excited state bound to partially oxidized Ru^{III}. A slight shift to higher energy is also observed for bipyridine bands in the RR spectrum of $[Ru^{III}(bpy)_3]^{3+}$ compared to $[Ru^{II}(bpy)_3]^{2+}$.[15]

The TRIR spectrum of $[Ru(bpy)_3]^{2+}$* (Table 3) can be assigned with one set of five bands originating from $bpy^{\bullet-}$ and a second set of five bands from the ancillary ligands. This provides clear, unambiguous evidence for the localized description of $[Ru^{III}(bpy^{\bullet-})(bpy)_2]^{2+}$*, at least in the lowest-lying MLCT excited state(s) on the ∼100 ns time scale.

(15) Woodruff, W. H. Personal communication.

Conclusions

The time-resolved infrared data on $[Re(bpy)(CO)_3(4\text{-Etpy})]^{+}$* and $[Ru(bpy)_3]^{2+}$* in the bipyridyl region provide previously unavailable band energies for asymmetric, excited-state vibrational modes for both chromophoric bpy and ancillary CO, bpy, and 4-Etpy ligands, which act as spectators to the $Re^{II}(bpy^{\bullet -})$ or $Ru^{III}(bpy^{\bullet -})$ interaction. The data complement those on totally symmetric modes obtained earlier by RR and TR[3].

For $[Ru(bpy)_3]^{2+}$* on the ∼100 ns time scale, there is clear, unambiguous evidence for localization with one partially reduced bpy and two ancillary bpy ligands bound to partially oxidized Ru^{III} in the excited state. The slight differences in ν(bpy) band energies between $[Ru(bpy)_3]^{2+}$*, $[Ru^{III}(bpy)_3]^{3+}$, and $[Ru^{II}(bpy)_2(bpy^{\bullet -})]^{+}$ are due to differences in polarization and back-bonding interactions between the ligands and the metal, which exist as Ru^{III} or Ru^{II} in the ground state, but is partially oxidized in the excited state.

This is the first study in which TRIR has been applied to the fingerprint region of an organometallic or transition metal complex excited state. It is a significant advance for TRIR spectroscopy, presaging the application of this technique to a wide range of organic and inorganic excited states. Limitations in the spectral region in the current study were imposed by the experimental conditions, and arose from solvent absorption and interference by optical components, not by the technique itself. Future studies will focus on expanding the spectral region to 500 cm^{-1}, improving the signal-to-noise ratio, and moving to shorter time scales.

Acknowledgment. This work was performed in part at Los Alamos National Laboratory under the auspices of the U.S. Department of Energy and was supported by Laboratory Directed Research and Development project No. 95101 to J.R.S. Work at the University of North Carolina was supported by the U.S. Department of Energy under Grant No. DE-FG02−96ER to T.J.M. The authors also wish to thank Dr. William H. Woodruff for helpful discussions.

JA970511U